Resonant Tunneling THz Oscillator at Fixed Bias Voltages

Peiji Zhao and H. L.Cui*
Department of Physics and Engineering Physics
Stevens Institute of Technology, Hoboken, NJ 07030, USA.
*Email: hcui@stevens-tech.edu

D. Woolard
Army Research Office, RTP, NC 27709, USA

Resonant tunneling diodes (RTD) have been studied as high frequency oscillators for many years.[1]~[5] Traditionally, RTD's are implemented purely as a negative differential resistance element with one energy storage element, the device capacitance. In terms of this design approach, oscillations must be generated by limit-cycles which exchange energy with resonating elements residing in the external bias circuit. This approach of extrinsically inducing oscillations will always encounter output power restrictions by external looses and low frequency design constraints. At the begin of the 90's, Jensen and Buot, in their numerical simulation of a double barrier quantum well system, found that there are intrinsic high frequency current oscillations in RTD. [4] The current oscillations are independent of external circuit. Their results provide evidence for a possible intrinsic approach to high frequency power generation. However, the causes of the intrinsic current oscillations are not clear for about ten years. It is very important to understand the causes of the oscillations since they are important to the intrinsic approach of design of the THz RTD oscillators. In this paper, we will explain the operational principle of the intrinsic THz RTD oscillators, the origin of the intrinsic high frequency current oscillations.

Our explanation of the origin of intrinsic high frequency oscillations is based on our numerical simulation of a resonant tunneling diode. The device model of our RTD is composed of the coupled Wigner –Poisson equations,

$$\frac{\partial f}{\partial t}+\frac{hk}{2\pi m^*}\frac{\partial f}{\partial x}+\frac{2}{\pi}\int_{-\infty}^{\infty}dk'\int_{0}^{\infty}dy\sin(2y(k-k'))\{V(x-y)-V(x+y)\}\cdot f(x,k',t)+\left[\frac{\partial f}{\partial t}\right]_{coll} \quad (1)$$

and

$$\frac{d^2u}{dx^2}=\frac{q^2}{\varepsilon}(N_d(x)-n(x)) \quad (2)$$

The parameters used in our simulation are the following. Momentum and position space is broken into 72 and 86 points, respectively. The donor density is 2×10^{18} particles/cm^3; the compensation ration for scattering calculations is 0.3; the barrier and well widths are 30 and 50 angstrom, respectively; the simulation box is 550 angstrom; the barrier potential is 0.3eV, corresponding to $Al_{0.3}Ga_{0.7}As$; the device temperature is 77K; the effective mass of electron is assumed to be a constant and equals to $0.0667m_0$; the

doping extend to 30 angstrom before the emitter barrier and after the collector barrier; the quantum-well region is undoped. Bulk GaAs parameters are used to calculate the relaxation time and the chemical potential. The chemical potential is determined by $\int_0^\infty d\varepsilon\sqrt{\varepsilon}f(\varepsilon)=\frac{2}{3}\mu(T=0)^{3/2}$, where $f(\varepsilon)$ is the Fermi distribution function. The relation time used in this paper is 525fs at 77K.

Fig.1 shows the calculated I-V characteristics of the structure used in this paper. This

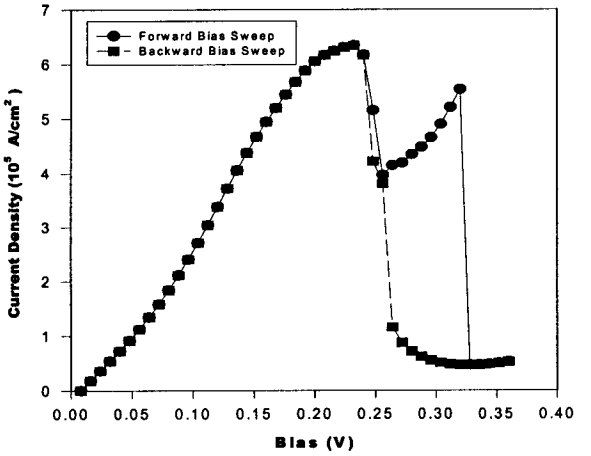

Fig.1 I-V characteristics of RTD. The data are taken from the steady states of the simulation. The values of the current in the BVW are calculated from time-average of the current oscillation.

figure shows all main features of the experimental results: a plateau-like structure and two hysteresis regions. This figure convinces us the correctness of our numerical calculation. Fig.2 shows the relationship between current density and simulation time. From this graph we know that there is a bias voltage window (BVW) in which the current density is oscillatory. The center bias voltage (CBV) of the bias window for the resonant tunneling structure (RTS) employed in this paper is 0.248V. At this bias voltage, the current oscillation is harmonic. Simulation results show if bias voltage is lower than the CBV, the current experiences a damping process at first and then develops into oscillated state. If the bias voltage is grater than the CBV in the BVW, the current densities do not show the initial damping and then harmonic oscillation process that can be observed when bias voltage is less than the CBV. The current gets into a damping process directly with a big initial amplitude. These are the basic features of the current oscillations in the RTS.

Fig.3 shows time-dependent self-consistent potential and electron density at 0.248V . We can see that the current oscillation is concurrent with those of potential and electron density in the whole region of the device. Except the oscillations of potential and density of electron in the whole region of the device, there is emitter quantum well (EQW) in front of the emitter barrier. Of course, the bottom of the EQW oscillates with the increase of the simulation time. Obviously, the current oscillation is related to the creation of an EQW. In our recent paper, we have presented large amount of figures showing the potential and density distribution of electrons in the device. These figures

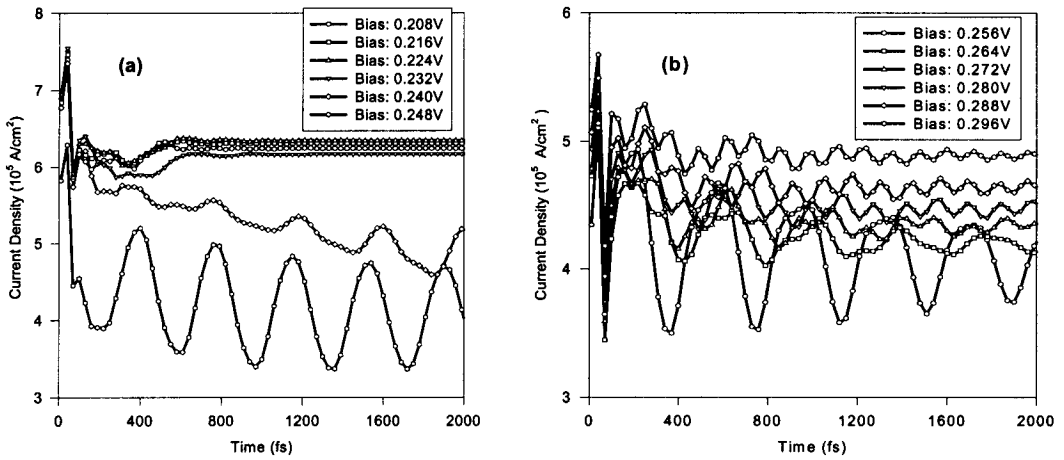

Fig.2 Current-time characteristics of the RTD with bias voltages as parameters in the case of forward bias sweep

and Fig.3 show that the oscillations have the following features. Before the bias get into the BVW, the potential and electron density just irregularly oscillate a short time and then get into stationary state. When the bias just enters the BVW, the potential vibrate a short time before getting into stable oscillation state. The oscillations are

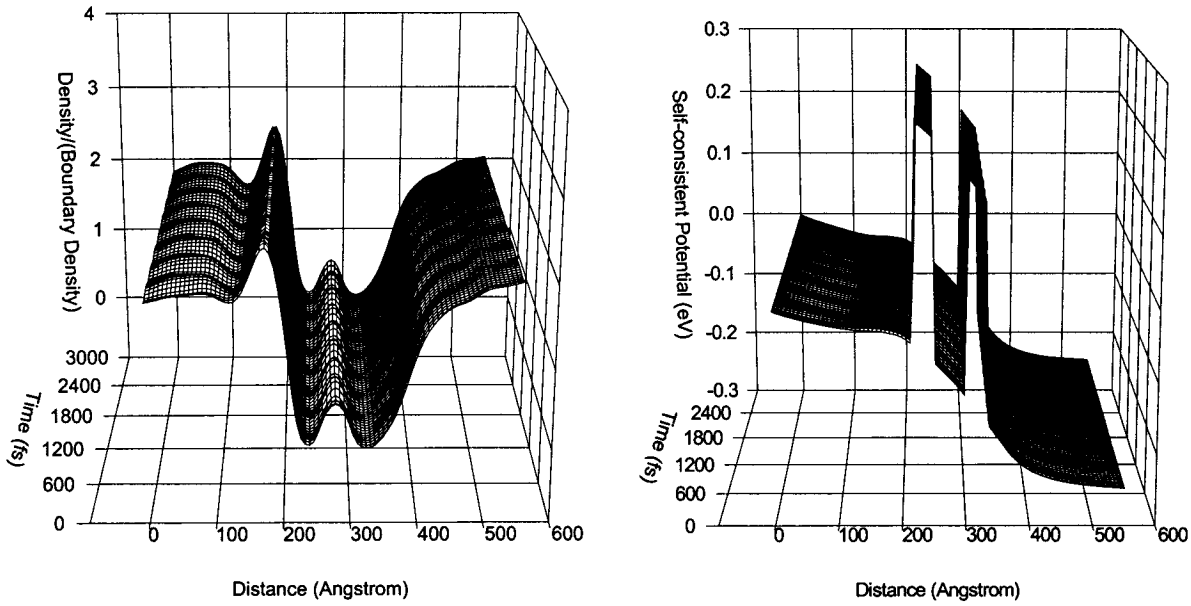

Fig.3 Time-dependent electron density distribution and self-consistent potential at bias voltage 0.248V. The figures show the oscillation of potential and density distribution in stable states. It should be noted that the depth of the EQW is increasing.

periodical rather than irregular. In the BVW, the irregular oscillations of the potential and electron density last a very short time. The potential and electron density get into stable oscillation quickly. After the bias voltage get out of the BVW in the higher bias voltage direction, the current oscillation become a decay oscillation, so do the potential and electron density. These situations last until the bias voltage reaches a special point where the plateau-like structure in the I-V characteristics ended. The oscillation features of potential and density are the same as that of current density stated above.

As we have stated, the oscillation of current is closely related to the creation of an EQW, so do those of potential and density distributions. It is very important to note that the EQW is created just after the current passes the maximum value of the current. Once the current passes the maximum value of the current, the reflection coefficient of the injected electron-wave increases dramatically. Thus, the interference between the injected electron-wave and the reflected electron-wave leads to depletion of electrons in front of the emitter barrier. The depletion of electrons in front of the emitter batter further leads to a relatively positive charge background thereby an EQW. Once the EQW is created and the energy level in the EQW is separated from the three dimensional states in the emitter, the coupling between the energy level in the EQW and that in the main quantum well will causes the oscillation of current through the double barrier system. Suppose that the wavefunctions for the energy levels in the EQW and the main quantum well (MQW) are expressed respectively as

$$\psi_{EQW}(z,t) = A(z)e^{i2\pi E_{EQW}t/h} \tag{3}$$

and

$$\psi_{MQW}(z,t) = B(z)e^{i2\pi E_{MQW}t/h-\gamma t}. \tag{4}$$

The γ factor in Eq.(4) stands for damping caused by electron-phonon interaction. We introduce this factor to the wave-function to reflect the following facts: the energy level in the MQW is next to the three dimensional states of electrons in the emitter and the width of the level is wider than that of the level in the EQW. The value of γ increases with the increase of the applied bias voltage. The total wave function can be expressed as

$$\psi = c_1\psi_{EQW} + c_2\psi_{MQW} \tag{5}$$

Thus, the current density and electron density can be written, respectively, as

$$<\psi \mid j \mid \psi>=\mid C_1 \mid^2 <A \mid j \mid A> + \mid C_2 e^{-\gamma t} \mid^2 <B \mid j \mid B> +2\,\mathrm{Im}(C_1^* C_2 <A \mid j \mid B>) e^{i2\pi(E_{MQW}-E_{EQW})t/h-\gamma t} \tag{6}$$

and

$$<\psi \mid \psi>=\mid c_1 \mid^2 <A \mid A> + \mid C_2 e^{-\gamma t} \mid^2 <B \mid B> +2\,\mathrm{Im}(C_1^* C_2 <A \mid B>) e^{i2\pi(E_{MQW}-E_{EQW})t/h-\gamma t} \tag{7}$$

These two equations fully reflect all main features of the simulation results. In Eq.(6), the first term sets the current value at which the oscillation is surrounded at steady states. The second term stands for the damping of the irregularly initial oscillation. The third term represents the oscillation of the current. Separated calculation shows $\Delta E = E_{MQW} - E_{EQW} \sim 10meV$ in BVW. Thus, the current oscillation frequency is in the order of 1THz that coincides with the simulation results shown by Fig.2. In fact, the strength of the oscillations depends on the strength of the coupling between the energy levels and that of the electron-phonon interaction. When bias voltage is small, $e^{-2\gamma t}$ factor destroys contributions from the second term in Eq.(6) smoothly. However, with the

increase of the depth of the EQW, the strength of the coupling between the two levels increases. The increase of the coupling leads to the increase of the amplitude of the oscillated currents. If this fact balances the effect of electron-phonon interaction, we get a harmonic current oscillation, such as shown by the current oscillation at 0.248V in Fig.2. If the strength of electron-phonon interaction is strong enough, the contribution from the second in Eq.(6) is quickly damped and the influence from $e^{-\eta t}$ in the third term in Eq.(6) gets into effects. This effect is greater at higher bias voltages. Fig.2 confirms our analysis. At bias voltage 0.248V, the self-consistent potential and electron density distribution all exhibit oscillation behaviors. The oscillation of electron density can be qualitatively explained by Eq.(7).

Our simulation results show that there is only one bias voltage region for the device structure employed in this paper in which the current oscillated. With the increase of bias voltage, electron-phonon interaction destroys the current oscillations. Since the structure used in this paper dose not allow another energy level to be created in the EQW, the EQW will collapse once the energy levels exchange their position. The exchange of the position of energy levels leads to the collapse of the EQW and the dramatic decrease of charge density in the main quantum well. The interaction between electron-phonon which dissipates electrons into the EQW, the interaction between the energy levels in the EQW and that in the main quantum, and the applied electric field which drives electrons into the EQW also contribute to the collapse of the EQW and the decrease of the charge density in the MQW. In fact, if the device structure is suitable for the creation of another energy level in the EQW, there will be another bias voltage region in which the current oscillates. [6]

In summary, we have pointed out the operational principle of a THz oscillator in an intrinsic approach. The operation of this kind of oscillators is not relied on external circuit but the intrinsic behavior of micro-particles, the wave behavior. The origin of the current oscillation is traced to the development of a dynamic emitter quantum well and the coupling of its energy level with the level of the main quantum well.

Reference:

[1]. R. K. Mains and G. I. Haddad, J. Appl. Phys. **64**, 3564(1988).
[2]. G. Frazier, A. Taddiken, A. Seabaugh, and J. Randall, IEEE Academic International Solid State Circuits Conference, TP 11.4 (1993).
[3]. E. R. Brown, in Hot Carriers in Semiconductor Nanostructures (edited by J. Shah), pp469, Academic Press, Boston, 1992; T. C. L. G. Sollner, E. R. Brown, W. D. Goodhue, and H. Q. Le, Appl. Phys. Lett. **50**, 332(1984).
[4]. K. L. Jensen and F. A. Buot, Phys. Rev. Lett. 66,1078(1991).
[5]. Peiji Zhao, H. L. Cui, and D. Woolard, submitted to Phys. Rev. B.
[6]. Peiji Zhao, H. L. Cui, and D. Woolard, submitted to IEEE/Cornell Conference on AdvConcepts in High Speed Semiconductor Devices & Circuits,2000.